Analytical Analysis of Flat Plate Solar Collector Integrated with Heat Pipes

Vivek Rai[1], Prof. Ashish Chaturvedi[2]

[1]*Student,* [2]*Assistant Professor*

[1]*Thermal Engineering, Oriental College of Technology (RGPV), Bhopal, India*

Abstract: ***Based on the heat transfer characteristics of absorber plate of a solar collector and the heat transfer effectiveness number or NTU method used for heat exchanger analysis, a new theoretical model for analysing the thermal performance of flat plate solar collector integrated with heat pipes has been put forward and the results have been validated by comparisons with the experimental results available in the literature. The theoretical model has been analysed and the results have been obtained for the specified values of input parameters by developing a MATLAB programme. The influence of relevant parameters on the thermal performance of flat plate solar collector integrated with heat pipes has been discussed. The proposed theoretical model can be helpful for a designer to design a new solar heating system integrated with the heat pipes for a better performance.***

Key words- Heat transfer characteristics, NTU method, Heat Pipes, MATLAB programmer.

I. INTRODUCTION

Solar thermal utilization is of nice importance visible of environmental protection and traditional energy saving. a spread of flat plate star collectors and exhausted hollow star collectors are created and applied round the world. However, these standard star collectors suffer from some inherent drawbacks, akin to reversed cycle throughout cloudy periods of the day and also the night, high pumping necessities, scale formation, freeze and corrosion [1].

Heat pipes supply a promising resolution to the higher than issues of standard collector Heat pipes square measure devices of terribly high thermal electrical phenomenon, that transfer thermal energy by 2 section circulation of fluid, and might simply be integrated into most sorts of solar furnace [2, 3]. The fundamental distinction within thermal performance between a heat pipe solar furnace and a standard one lies in the heat transfer processes from the absorbent surface to the energy-transporting fluid. within the case with a heat pipe, the method is evaporation–condensation–convection, whereas for standard star collectors, heat transfer happens solely on the absorbent plate. A feature that creates heat pipes engaging to be used in star collectors is their ability to control sort of a thermal-diode, i.e., the flow of the warmth is in one directional. This minimizes heat loss from the transporting fluid, e.g., water and air, once incident radiation is low. Another advantage is redundancy, that is, a failure in one heat pipe wouldn't have a serious result on the operation of the collector. Also, since heat pipes square measure sealed, by choosing appropriate operating fluids, compatible with wick and pipe materials, corrosion is decreased . moreover, once the most style temperature of the collector is reached, further heat transfer is prevented. this is able to stop warming of the current fluid. freeze is eliminated through operating fluid choice, and, so solely the warmth money dealer section should be insulated.

II. METHODS

1. Methodology

In this chapter mathematical & computational modelling has been done using basic energy balance equations and NTU method of heat exchanger analysis and equations have been solved using appropriate boundary conditions. The generalised energy balance equations are obtained which can be used for calculating the temperature of heat pipe surfaceand the temperature of heated fluid at outlet, as it flows past the heat pipes. The Equation can be used to obtain system efficiency under different environmental conditions and system geometry.

(a)

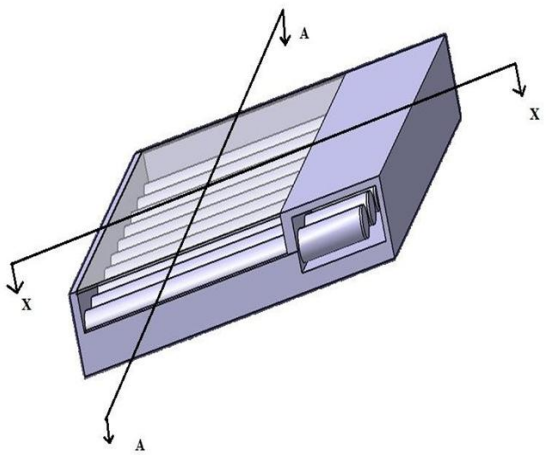

Fig. 1 (a) Physical model of flat plate solar collector integrated with heat pipes.

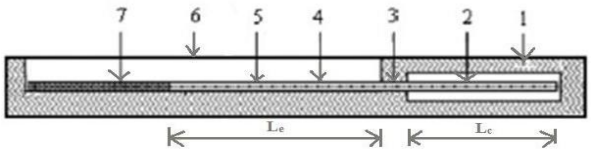

1-Insulation; 2-Condensor section; 3-Adiabatic section;
4-Evaporator section; 5-Heat pipe; 6-Glass cover;
7-Working fluid of heat pipe

(b)

Fig.1 (b) Section X-X of the physical model (c)

Io

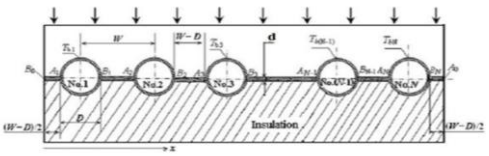

Fig.1 (c) Section A-A of the physical model

Figure 1(a), 1(b) & 1(c) show a flat plate solar collector integrated with numbers of wickless heat pipes. The evaporator sections with length Le of the wickless heat pipes are welded to absorber plate made of copper sheets. The condenser sections with length Lc of the wickless heat pipes are immersed in a cooling manifold. The pitch distance between the heat pipe is W, the heat pipe diameter is D and the absorber plate thickness is d. The absorber plate and heat pipe are made of copper, and the thermal conductivity of which is k. The left and right sides of absorber plate which contain point B0 and A0 respectively are adiabatic walls.

The ambient temperature is Ta. Solar intensity is Io, while the solar energy intensity absorbed by absorber plate is S (without glass cover: S = Io(α); with glass cover: S = Io(ατ), where α is absorptivity of absorber plate and heat pipe wall, τ is transmissivity of glass cover). The wall temperature of each heat pipe region A1–B1, A2–B2, A3–B3… AN– BN is assumed to be uniform, which are Tb1, Tb2, and Tb3…TbN. All these temperatures are unknown and require to be solved.

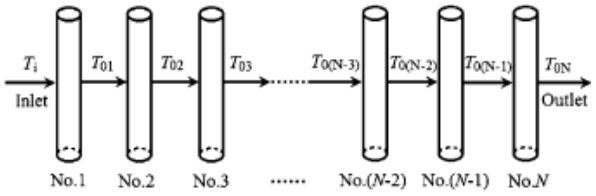

Fig. 2 Temperature at various points of heated fluid in the condenser section of heat pipe

As displayed in Fig. 2, for a collector with N heat pipes, the heated fluid flows orderly through the condenser sections from the 1stheat pipe to the Nth one in a crosswise manner. The heated fluid outlet temperature of the 1stcondenser section of heat pipe equals to the heated fluid inlet temperature of the 2ndone, and so on. The final temperature of heated fluid through N heat pipes is T0N, which needs to be solved, and the heated fluid inlet temperature Ti is a known quantity.

2.2 Theoretical Analysis

- To develop the energy balance equations and to get its solution for the heat pipe collector as shown in Fig. 1(c), the following assumptions have been made:
- The system is in quasi-steady state.
- The phase change of the working fluid inside the wickless heat pipe occurs at approximately constanttemperature and the temperature difference between the evaporator and condenser sections of the heat pipe is less than 2.
- The thickness of absorber plate with high heat conduction performance is much less than the width, so the temperature variation along the thickness of absorber plate is negligible.
- The overall heat loss coefficient between the absorber plate of collector and the external environment is treated as a constant.
- The heat pipe collector is well insulated and the heat loss through the insulation is neglected. Meanwhile, both end sides of the absorber plate are adiabatic.
- Since the absorber plate is made of copper which is good conductor of heat, the temperature gradient of the absorber plate along the axial direction of heat pipe is negligible, therefore the heat transfer process in the regions

B0–A1, B1–A2, B2–A3,… BN–A0 of absorber plate is similar to the heat conduction problem of a fin.

Heat Flow in region B0–A1 (Fig.1 (c))

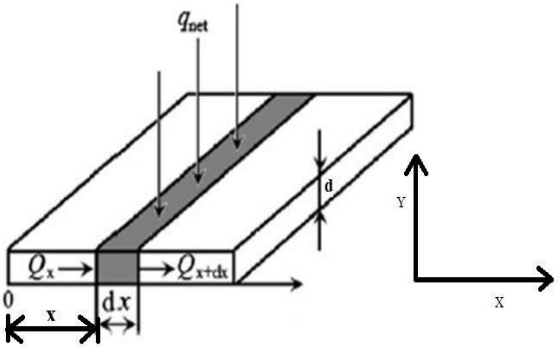

Fig. 3 The heat transfer process in B0–A1 region of absorber plate

Referring to Fig.1(c) the one-dimensional steady-state heat conduction of a fin with width of(W - D)/2 is taken for the heat transfer process in the region B0–A1 of absorber plate. A differential element with width of dx, at a distance x from the left end as shown in Fig. 3, is taken to analyse the energy balance. The assumption that the length of collector along the axial direction of heat pipe is set to be 1 is made. The net input heat rate from the solar irradiation Qnet is

Qnet=qnetdx=[S-UL(T-Ta)]dx (1)

Where

qnet is the net input heat flux;

UL is the collector overall heat loss coefficient;

T is surface temperature of fin at a distance x from the left side.

In terms of the heat transfer analysis of B0–A1 region, the heat transfer direction is parallel to +x axis, thus the energy balance of the differential element control volume in Fig. 3 as a whole gives

Qx+Qnet= Qx+dx (2)

In accordance with Fourier's law of heat conduction and in combination with Eq. (1), (2) would be

$$\frac{d^2T}{dX^2} + \frac{U_L(T-T_a)}{kd} = 0 \quad (3)$$

The general solution of Eq. (3) is

T=C01emx+C02e-mx+S/(U_L+T_a) (4)

Where C01 and C02 are integration constants and

$$m = \sqrt{\frac{U_L}{kd}}$$

The corresponding boundary conditions (the point B0 is coordinate origin) are

dT/dx=0, at x=0

And T = Tb1, at x = (W-D)/2 (5)

Thus

$$C01 = C02 = \frac{T_{b1} - \frac{S}{U_L + T_a}}{2\cosh m\frac{H}{2}} \quad (6)$$

Where H = W - D.

Substituting Eq. (6) into Eq. (4), the final solution for the temperature distribution is then

$$T = \frac{\cosh mx}{\cosh m\frac{H}{2}}\left(T_{b1} - \frac{S}{U_L + T_a}\right) + \frac{S}{U_L + T_a} \quad (7)$$

The heat flow rate which enters into the vertical plane that contains point A1 by conduction can be expressed as

QA1=-kdLedT/dx

At x=H/2,

QA1¬= 0.5HLeηf[S-U_L(Tb1-Ta)] (8)

Where ηf is the standard fin efficiency for straight fins with rectangular profile,

Obtained from

$$\eta f = \frac{\tanh\frac{mH}{2}}{\frac{mH}{2}}$$

Heat Flow in region B1–A2(Fig 1(c))

When the heated fluid flows through the condenser of the 1stheat pipe to the Nthone successively, the temperature of heated fluid gradually goes up. Accordingly, the working fluid temperature of heat pipe rises up, from Thp1 to Thpn. Heat flow directions of the regions B1–A2, B2–A3, B3–A4, …, BN-1–AN are reverse to +x- axis.

In a similar manner, the heat transfer process in region B1–A2 of absorber plate can be considered as one dimension steady-state heat conduction problem of a fin with width of (W - D). Combining the thermal conduction equation Eq. (3) with boundary conditions

x = 0, T = Tb1;

x = W - D, T = Tb2,

The integration constants of Eq. (4) are obtained as

$$C_{12} \frac{T_{b1} - \frac{S}{U_L + \mathrm{Ta}}\exp mH}{2\sinh mH} - \frac{T_{b2} - \frac{S}{U_L + \mathrm{Ta}}}{2\sinh mH'}$$

and

$$C11 = Tb1\text{-}C12 - \frac{S}{U_L + \mathrm{Ta}} \quad (9)$$

The heat flow rate into the vertical plane that contains point B1 is calculated by

QB1=-kdLedT/dx

At x=0

$$QB1 = -kdmLe\left[Tb1\text{-}2C12 - \frac{S}{U_L - \mathrm{Ta}}\right. \quad (10)$$

On the basis of the temperature distribution of region B1–A2 in absorber plate, the heat flow rate out of the vertical plane that contains point A2 is written as

QA2=-kdLedT/dx

Atx= W-D

QA2=-kdmLe[C11e^mH- C12e^(-mH)] (11)

Heat flow in region A1–B1 of No.1 heat pipe(Fig 1 (c))

The gain in solar energy in the region A1–B1 of No.1 heat pipe is

QA1B1=(π/2)DLe[S-UL(Tb1-Ta)] (12)

The useful energy obtained by the No.1 heat pipe is

Qhp1 = GCp(T01–Ti)(13)

Where T01 is heated fluid outlet temperature of No.1 heat pipe. (13)

The energy balance of the region A1–B1 of No.1 heat pipe as a whole gives

QA1 + QA1B1 +|QB1| = Qhp1(14)

Then the following equation can be obtained,

$$0.5\,H\,L_e\,\eta_f\,S - U_L\,T_{b1} - T_a + \frac{\pi}{2}D\,L_e\,S - U_L\,T_{b1} - T_a + k\,d\,m\,L_e\,T_{b1} - 2C_{12} - \frac{S}{U_L - T_a} = G\,C\,T_p - T_{01}\quad i$$

Equation (15) contains unknown temperature Tb1, Tb2, T01.

Heat flow in region An–Bn of No.n (n = 2, 3, 4,…,N-1) heat pipe(Fig 1 (c))

For the region An–Bn of No.n (n = 2, 3, 4,…,N-1) heat pipe, the heat transfer process of each region is similar. Applying the analysis method of the region A1–B1, we also have

$$\frac{\pi}{2}D\,L_e\quad S - U_L\;T_{bn} - T_a + k\,d\,m\,L_e\quad [T_{bn} - 2C_{n2} - S/(U_L - T_a)] = GC_p\,(T_{0n} - T_{0(n-1)}) + kdmL_e\,[\,C_{n-1\,1}e^{mH} + C_{n-1\,2}e^{-mH}$$

Where

$$C(n-1)2 = T_{b\,n-1} - \frac{S}{U_L+T_a}\;\frac{e^{mH}}{2sinh\;m\;H} - \frac{T_{bn} - \frac{S}{U_L+T_a}}{2sinh\;m\;H}) \quad (17.1)$$

$$C(n-1)1 = Tb(n-1) - C(n-1)2 - \frac{S}{U_L + T_a} \quad (17.2)$$

$$Cn2 = \frac{T_{bn} - \frac{S}{U_L+T_a}\;e^{mH}}{2sinh\;m\;H} - \frac{T_{b\,n+1} - \frac{S}{U_L+T_a}}{2sinh\;m\;H} \quad (17.3)$$

(14)

In which, Tb(n-1) is the region An-1–Bn-1 temperature of No.(n – 1) heat pipe; Tbn is the region An–Bn temperature of No.n heat pipe Tb(n+1) is the region An+1–Bn+1 temperature of No.(n + 1) heat pipe; T0(n-1) is heated fluid inlet temperature of No.n heat pipe. T0n is heated fluid outlet temperature of No.n heat pipe. Among these, Tb(n-1), Tbn, T0(n-1) and T0n are unknown.

Heat flow in region AN–BN of No N heat pipe

Since the analysis method of the region AN–BN of NoN heat pipe is almost the same as that of the region A1– B1 of No.1 heat pipe except for different boundary conditions, thus neglected for brevity's sake. The right side surface of absorber plate is adiabatic.

The appropriate boundary conditions (the point BN is coordinate origin) would be

T=TbN at x=0;

dT/dx=0 at x=(W-D)/2 (18)

Therefore, application of the above boundary conditions yields the integration constants of general solution Eq. (4) as

$$CN1 = \frac{T_{bN} - \frac{S}{U_L+T_a}}{1+e^{mH}}, \text{ and}$$

$$CN2 = TbN - CN1 - \frac{S}{U_L + T_a} \quad (19)$$

The heat flow rate into the vertical plane that contains point BN is calculated by

QBN=-kdLedT/dx

At x=0

QBN= -kdmLe(CN1-CN2) (20)

The energy balance equation for the region AN–BN of No N heat pipe is written as

|QBN| =QANBN =|QA| +QhpN (21)

Where QANBN is the gained solar energy in the region AN– BN of No N heat pipe; QAN is the heat flow rate out of the vertical plane that contains point AN. The useful energy gained by the No.N heat pipe is given by

QhpN=GCp(T0N-T0(N-1)) (22)

Combining Eq. (20), (21) and (22) leads to:

$$k\,d\,m\,L_e\;\;2C_{N1} - T_{bN}\;\; + \frac{S}{U_L + T_a} + 0.5\,\pi\,D\,L_e\,S - U_L\,T_{bN} - T_a = G\,C_p\,T_{0N} - T_{0\,N-1} + k\,d\,m\,L_e\,C_{N-1\,1}e^{mH} - C_{N-1\,2}e^{-mH}$$

It is clear that Eq. (23) contains unknown temperature TbN-1, TbN,T0(N-1) and T0N.

The relation between T0n&Tbn

For No.1 heat pipe, the heat transfer effectiveness E1 and the number of heat transfer unit NTUc1are defined as

$E1 = 1 - e^{-NTU_{c1}}$;

$$NTU_{c1} = \frac{A_{c1} U_{c01}}{G\, C_P} \quad (24)$$

Where U_c01 is heat convection coefficient of heated fluid and the condenser section, it can be obtained from Nu = 0.26Re^0.6 Pr^(1/3) [22]; Ac1 is the heat exchange area of heated fluid and the condenser section of heat pipe.

From $E1 = \frac{T_{01} - T_i}{T_{c01} - T_i}$ we have

$$T01 = Ti + 1 - e^{-NTUc1}\, T_{c01} - T_i \quad (25)$$

(16)

where Tc01 is the working fluid temperature of No.1 heat pipe condenser section and equal to the working fluid temperature of No.1 heat pipe Thp1. Considering that phase transition heat transfer coefficient of heat pipe is rather high, and the temperature difference of phase transition heat transfer is much smaller than that of single phase convection heat transfer, namely, Tc01 = Thp1& Tb1. Therefore, Eq. (25) may be rearranged in the following form:

T01 = Ti +(1-e^(-NTUc1))(Tb1–Ti) (26)

Proceeding in a similar fashion, for No.n heat pipe (n = 2, 3, 4,…, N), it is readily shown that

T0n = T0n-1+(1-e^(-NTUcn)) (Tbn-T0n-1) (27)

Again, En = 1-e^(-NTUcn);

$$NTUcn = \frac{A_{cn}\, U_{cn}}{G\ \mathrm{Cp}} \quad (28)$$

It is assumed that each heat pipe is the same, namely ACn = AC1, UCn = UC1, we have

E1 =E2 =E3 =E4 ==En =E (29)

From Eq. 26 to 29, the following equations are obtained:

T01 = Ti + E (Tb1–Ti)

= E Tb1 +(1 - E)Ti (30)

T02 = E Tb2 +(1 - E) E Tb1+(1-E)^2Ti (31)

T0n = Ti(1-E)^n+(1-E)^(n-1)E Tb1 +(1-E)^(n-2)E Tb2 +… .....+(1- E) E Tbn-1+

E Tbn (32)

(17)

From the relation T0N with TbN, it is shown that Eq. (15), (16) and (23) consist of N equations which contain N unknown quantities. Obviously, closed form solutions can be obtained from these equations. Namely, we can gain the temperature Tb1, Tb2, Tb3,…,TbN of region A1–B1, A2–B2, A3–B3,…, AN–BN of the heat pipes. Meanwhile, the heated fluid outlet temperature of each heat pipe T01, T02, T03,…, T0N can be found out.

Further, the thermal efficiency of the heat pipe flat plate solar collector η can be calculated as [7]

$$\eta = \frac{G\, C_p\, T_{0N} - T_i}{I_o\ A_c} \quad (33)$$

Where Ac is area of collector,

Ac= NWLe.

III. RESULT AND DISCUSSION

Heat pipe made of copper with length of 0.92 m and outer diameter D of 0.0127 m is used. Lengths of evaporator and condenser section, i.e., Le and Lc are 0.75m and 0.1 m, respectively. The glass cover plate is sized in 0.76 m x 1.9 m x 0.004 m, of which the transmissivity τ is 0.9. The absorber plate is made of copper with size of 1.89 m x 0.75 m and it is coated with anodic alumina spectral selective absorption material of which the absorptivity α is 0.94. The condenser section of heat pipe is placed in the heated fluid channels of 1.9 m x 0.1 m x 0.03m. The heat loss coefficient between the absorber plate and environment UL is 8.6 Wm-2 K-1[23]. Other parameters, such as solar intensity Io and ambient temperature Ta are taken as [7].

A CPP Programme has been developed and used to solve above equations and results are listed in the form of Tables and Plots

3.2 Results & Discussion

Table 3.1.1 Values of Io, Ti and Ta with respect to timeat Cairo, Egypt

S.N.	Time (hrs)	Solar Intensity I_o (Wm^{-2})	Heated Fluid Inlet Temperature T_i (^0C)	Ambient Temperature T_a (^0C)
1	10:00	600	38	28
2	11:00	700	39	30

3	12:30	800	42	34
4	14:00	790	43	34
5	16:00	550	44	35

(19)

Table 3.1.2 Heated water outlet temperature for G = 0.0229 kg/s

S.N.	Heated Fluid Outlet Temperature (^{0}C)	10:00 (hrs)	11:00 (hrs)	12:30 (hrs)	14:00 (hrs)	16:00 (hrs)
1	T_{01}	38.065865	39.080425	42.094990	43.092323	44.060604
2	T_{02}	38.274635	39.379086	42.471725	43.445610	44.199287
3	T_{03}	38.480320	39.673336	42.842896	43.793678	44.335922
4	T_{04}	38.682968	39.963238	43.208584	44.136604	44.470539
5	T_{05}	38.882622	40.248859	43.568871	44.474464	44.603168
6	T_{06}	39.079327	40.530262	43.923832	44.807335	44.733837
7	T_{07}	39.273125	40.807507	44.273552	45.135288	44.862576
8	T_{08}	39.464062	41.080654	44.618107	45.458397	44.989410
9	T_{09}	39.652176	41.349766	44.957569	45.776733	45.114372
10	T_{010}	39.837513	41.614902	45.292019	46.090366	45.237488
11	T_{011}	40.020111	41.876125	45.621529	46.399364	45.358788
12	T_{012}	40.200012	42.133488	45.946171	46.703800	45.478294
13	T_{013}	40.377254	42.387047	46.266014	47.003738	45.596035
14	T_{014}	41.662533	43.943111	48.096466	48.786758	46.794868

(20)

Table 3.1.3 Heated water outlet temperature for G = 0.0458 kg/s

S.N.	Heated Fluid Outlet Temperature (^{0}C)	10:00 (hrs)	11:00 (hrs)	12:30 (hrs)	14:00 (hrs)	16:00 (hrs)
1	T_{01}	38.032955	39.040241	42.047527	43.046192	44.030323
2	T_{02}	38.137173	39.189281	42.235504	43.222481	44.099613
3	T_{03}	38.240623	39.337223	42.422096	43.397472	44.168396
4	T_{04}	38.343311	39.484077	42.607315	43.571175	44.236671
5	T_{05}	38.445244	39.629852	42.791172	43.743599	44.304443
6	T_{06}	38.546429	39.774551	42.973679	43.914757	44.371719
7	T_{07}	38.646866	39.918186	43.154842	44.084656	44.438499
8	T_{08}	38.746567	40.060764	43.334671	44.253304	44.504787
9	T_{09}	38.845531	40.202293	43.513176	44.420712	44.570587
10	T_{010}	38.943771	40.342781	43.690369	44.586887	44.635902
11	T_{011}	39.041286	40.482239	43.866257	44.751839	44.700737
12	T_{012}	39.138084	40.620770	44.040852	44.915577	44.765095
13	T_{013}	39.234169	40.758083	44.214161	45.078114	44.828979
14	T_{014}	39.894264	41.560635	45.160103	45.998535	45.440544

(21)

Table 3.1.4 Heated water outlet temperature for G = 0.0916 kg/s

S.N.	Heated Fluid Outlet Temperature	10:00	11:00	12:30	14:00 (hrs)	16:00

	(^{0}C)	(hrs)	(hrs)	(hrs)		(hrs)
1	T_{01}	38.016483	39.020126	42.023769	43.023106	44.015167
2	T_{02}	38.068550	39.094574	42.117661	43.111160	44.049801
3	T_{03}	38.120426	39.168747	42.211205	43.198895	44.084309
4	T_{04}	38.172112	39.242649	42.304405	43.286304	44.118667
5	T_{05}	38.223606	39.316280	42.397266	43.373394	44.152939
6	T_{06}	38.274914	39.389641	42.489784	43.460163	44.187065
7	T_{07}	38.326031	39.462730	42.581963	43.546616	44.221066
8	T_{08}	38.376961	39.535553	42.673805	43.632748	44.254944
9	T_{09}	38.427704	39.608109	42.765308	43.718567	44.288696
10	T_{010}	38.478260	39.680397	42.856476	43.804070	44.322327
11	T_{011}	38.528629	39.752419	42.947308	43.889259	44.355831
12	T_{012}	38.578815	39.824177	43.037807	43.974136	44.389214
13	T_{013}	38.628819	39.895672	43.187975	44.058701	44.422474
14	T_{014}	38.963482	40.303432	43.609074	44.526558	44.731464

(22)

Table 3.1.5 Heated air outlet temperature for G = 0.0229 kg/s

S.N.	Heated Fluid Outlet Temperature (^{0}C)	10:00 (hrs)	11:00 (hrs)	12:30 (hrs)	14:00 (hrs)	16:00 (hrs)
1	T_{01}	38.273251	39.333656	42.394066	43.383007	44.251411
2	T_{02}	39.152248	40.593868	43.985001	44.874275	44.831970
3	T_{03}	39.975761	41.774532	45.475510	46.271412	45.375881
4	T_{04}	40.747292	42.880672	46.871933	47.580357	45.885460
5	T_{05}	41.470119	43.916988	48.180210	48.806679	46.362873
6	T_{06}	42.147320	44.887890	49.405907	49.955589	46.810150
7	T_{07}	42.781773	45.797504	50.554234	51.031979	47.229191
8	T_{08}	43.376179	46.649700	51.630074	52.040421	47.621780
9	T_{09}	43.933064	47.448105	52.638004	52.985207	47.989590
10	T_{010}	44.454796	48.196110	53.582310	53.870358	48.334183
11	T_{011}	44.943596	48.896900	54.467010	54.699635	48.657024
12	T_{012}	45.401539	49.553455	55.295864	55.476566	48.959488
13	T_{013}	45.830578	50.168564	56.072399	56.204456	49.242859
14	T_{014}	50.483017	55.667992	62.467850	62.473888	53.744987

(23)

Table 3.1.6 Heated air outlet temperature for G = 0.0458 kg/s

S.N.	Heated Fluid Outlet Temperature (^{0}C)	10:00 (hrs)	11:00 (hrs)	12:30 (hrs)	14:00 (hrs)	16:00 (hrs)
1	T_{01}	38.137005	39.167294	42.197582	43.192039	44.126057
2	T_{02}	38.573437	39.792193	42.985943	43.931225	44.415409
3	T_{03}	38.996323	40.397522	43.749836	44.647469	44.695778
4	T_{04}	39.406082	40.984150	44.490017	45.341480	44.967445
5	T_{05}	39.803123	41.552570	45.207226	46.013950	45.230682
6	T_{06}	40.187843	42.103348	45.902176	46.665550	45.485748
7	T_{07}	40.560623	42.637032	46.575554	47.296925	45.732899
8	T_{08}	40.921829	43.154152	47.228035	47.908703	45.972378

9	T_{09}	41.271828	43.655220	47.860264	48.501495	46.204422
10	T_{010}	41.610962	44.140736	48.472870	49.075886	46.429264
11	T_{011}	41.939571	44.611183	49.066460	49.632450	46.647129
12	T_{012}	42.257980	45.067028	49.641628	50.171741	46.858231
13	T_{013}	42.566505	45.508724	50.198944	50.694294	47.062782
14	T_{014}	45.103970	48.553890	53.766193	54.177124	49.462414

(24)

Table 3.1.7 Heated air outlet temperature for G = 0.0916 kg/s

S.N.	Heated Fluid Outlet Temperature (^{0}C)	10:00 (hrs)	11:00 (hrs)	12:30 (hrs)	14:00 (hrs)	16:00 (hrs)
1	T_{01}	38.068600	39.083763	42.098930	43.096153	44.063118
2	T_{02}	38.286072	39.394882	42.491383	43.464180	44.207573
3	T_{03}	38.500198	39.701214	42.877796	43.826542	44.349805
4	T_{04}	38.711029	40.002831	43.258263	44.183327	44.489845
5	T_{05}	38.918613	40.299805	43.632874	44.534618	44.627731
6	T_{06}	39.123001	40.592209	44.001720	44.880505	44.763496
7	T_{07}	39.324245	40.880112	44.364887	45.221066	44.897171
8	T_{08}	39.522392	41.163582	44.722466	45.556385	45.028786
9	T_{09}	39.717487	41.442692	45.074539	45.886457	45.158375
10	T_{010}	39.909580	41.717506	45.421196	46.211624	45.285973
11	T_{011}	40.098717	41.988091	45.762516	46.531700	45.411606
12	T_{012}	40.284943	42.254509	46.098583	46.846848	45.535305
13	T_{013}	40.468304	42.516827	46.429478	47.157146	45.657101
14	T_{014}	41.804077	44.133461	48.330878	49.009438	46.903713

(25)

Table 3.1.8 Efficiency of system using water as fluid for G = 0.0229 kg/s

Time (hrs)	Solar Intensity I_o (Wm^{-2})	Ambient Temperature T_a (^{0}C)	Heated Fluid Inlet Temperature T_i (^{0}C)	Heated Fluid Outlet Temperature T014 (^{0}C)	Thermal Efficiency η (%)
10:00	600	28	38	41.662533	41.290073
11:00	700	30	39	43.943111	47.765877
12:30	800	34	42	48.096466	51.547020
14:00	790	34	43	48.786758	49.547718
16:00	550	35	44	46.794868	34.372734

Table 3.1.9 Efficiency of system using water as fluid for G = 0.0458 kg/s

Time (hrs)	Solar Intensity I_o (Wm^{-2})	Ambient Temperature T_a (^{0}C)	Heated Fluid Inlet Temperature T_i (^{0}C)	Heated Fluid Outlet Temperature T014 (^{0}C)	Thermal Efficiency η (%)
10:00	600	28	38	39.894264	42.710503
11:00	700	30	39	41.560635	49.487438

12:30	800	34	42	45.160103	53.438786
14:00	790	34	43	45.998535	51.348457
16:00	550	35	44	45.440544	35.433105

(26)

Table 3.1.10 Efficiency of system using water as fluid for G = 0.0916 kg/s

Time (hrs)	Solar Intensity I_o (Wm^{-2})	Ambient Temperature T_a (^0C)	Heated Fluid Inlet Temperature T_i (^0C)	Heated Fluid Outlet Temperature T014 (^0C)	Thermal Efficiency η (%)
10:00	600	28	38	38.963482	43.447788
11:00	700	30	39	40.303432	50.380894
12:30	800	34	42	43.609074	54.420345
14:00	790	34	43	44.526558	52.283131
16:00	550	35	44	44.731464	35.983704

Table 3.1.11 Efficiency of system using air as fluid for G = 0.0229 kg/s

Time (hrs)	Solar Intensity I_o (Wm^{-2})	Ambient Temperature T_a (^0C)	Heated Fluid Inlet Temperature Ti (^0C)	Heated Fluid Outlet Temperature T014 (^0C)	Thermal Efficiency η (%)
10:00	600	28	38	50.483017	33.778999
11:00	700	30	39	55.667992	38.660168
12:30	800	34	42	62.467850	41.539444
14:00	790	34	43	62.473888	40.022484
16:00	550	35	44	53.744987	28.767166

(27)

Table 3.1.12 Efficiency of system using air as fluid for G = 0.0458 kg/s

Time (hrs)	Solar Intensity I_o (Wm^{-2})	Ambient Temperature T_a (^0C)	Heated Fluid Inlet Temperature T_i (^0C)	Heated Fluid Outlet Temperature T014 (^0C)	Thermal Efficiency η (%)
10:00	600	28	38	45.103970	38.446632
11:00	700	30	39	48.553890	44.319173
12:30	800	34	42	53.766193	47.758919
14:00	790	34	43	54.177124	45.942165
16:00	550	35	44	49.462414	32.250050

Table 3.1.13 Efficiency of system using water as fluid for G = 0.0916 kg/s

Time	Solar Intensity I_o	Ambient Temperature T_a	Heated Fluid Inlet Temperature T_i (^0C)	Heated Fluid Outlet Temperature T014	Thermal Efficiency η (%)

(hrs)	(Wm^{-2})	(^0C)		(^0C)	
10:00	600	28	38	41.804077	41.175278
11:00	700	30	39	44.133461	47.626720
12:30	800	34	42	48.330872	51.393948
14:00	790	34	43	49.009438	49.402077
16:00	(28)550	35	44	46.903713	34.286999

Using the values of solar intensity Io(W/m2) and time (hrs) from table 3.1.1 a graph has been plotted (Fig.4)

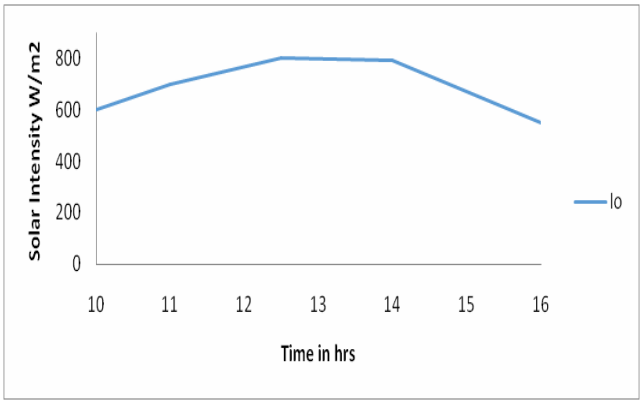

Fig. 4 Variation of Incident Solar Radiation with time

It can be seen from fig.4 that the value of solar intensity increase as time increases and reaches a maximum value of 800 W/m2 then starts decreasing

Using the values of ambient temperature Ta (oC), heated fluid inlet temperature Ti (oC) and time (hrs) from table 3.1.1 a graph has been plotted (Fig.5)

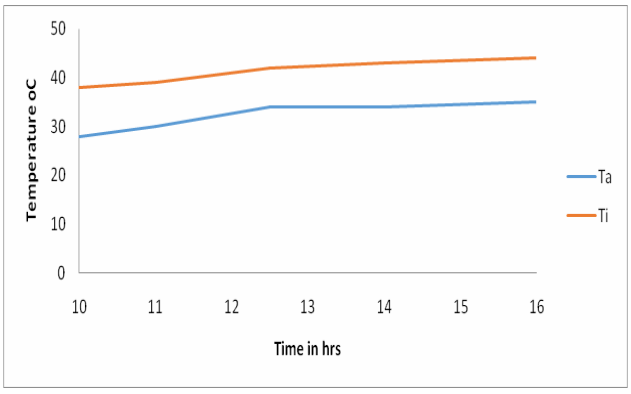

Fig. 5 Variation of ambient temperature and heated fluid inlet temperature with time

It can be seen from fig.5 that the value of ambient temperature and heated fluid inlet temperature increase as time increases and reaches a maximum value of 35 oC& 44 oC respectively.

(29)

Using the values of thermal efficiency η (%) for different mass flow rate of water G under different environmental conditions and time (hrs) from table 3.1.8, 3.1.9 & 3.1.10 a graph has been plotted (Fig.6)

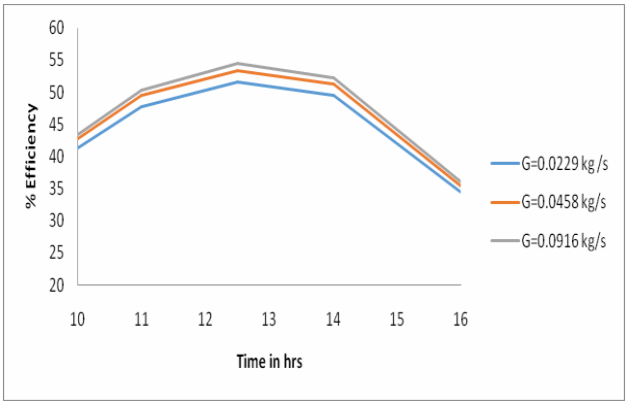

Fig. 6 Time v/s Efficiency Plot for Water

It can be seen from fig.6 that the value of thermal efficiency increases as time & mass flow rate increase and reaches a maximum value of 54.42% for the value of G = 0.0916 kg/s and then starts decreasing.

Using the values of thermal efficiency η (%) for different mass flow rate of air G under different environmental conditions and time (hrs) from table 3.1.11, 3.1.12 & 3.1.13 a graph has been plotted (Fig.7)

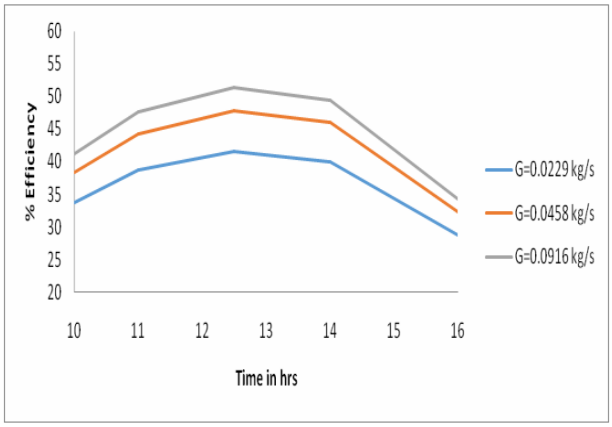

Fig. 7 Time v/s Efficiency Plot for Air (30)

It can be seen from fig.7 that the value of thermal efficiency increase as time & mass flow rate increases and reaches a maximum value of 51.39% for the value of G = 0.0916 kg/s and then starts decreasing.

Using the values of thermal efficiency η (%) for mass flow rate of water G = 0.0458 kg/s from table 3.1.9 and from Ref. [7]. under same environmental conditions and time (hrs) a graph has been plotted (Fig.8)

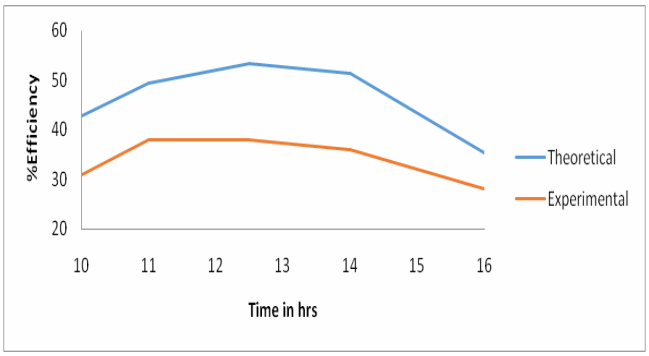

Fig. 8 Theoretical & Experimental Efficiency v/s Time Plot for Water for

G = 0.0458 kg/s

It can be seen from fig.8 that the value of theoretical and experimental thermal efficiency increase as time increases and reaches a maximum level then starts decreasing. From the fig.8 it can be seen that experimental efficiency is always less than that of experiment because of losseswhich are not considered in our analysis.

IV. CONCLUSION

On the basis of present analysis it is concluded that:

- The Efficiency of the system increases with increase in mass flow rate and increase in intensity of incident solar radiation in case of both fluids (Water & Air) .
- Maximum system efficiency obtained for water as a fluid is 54.42% corresponding to Values of Io= 800 W/m2 and G = 0.0916 kg/s.
- Maximum system efficiency obtained for air as a fluid is 51.39% corresponding to Values of Io= 800 W/m2 and G = 0.0916 kg/s.
- It is very much clear that for same mass flow rate and same environmental conditions system efficiency obtained for water as a fluid is more as compared to that of air as a fluid.
- The theoretical analysis proposed can be used for flat plate solar collector integrated with heat pipes design and assessment. It is an efficient approach to analyse and discuss the influences of solar intensity, water inlet temperature, environmental temperature, heated fluid mass flow rate and collector's parameters on the flat plate solar integrated with heat pipes performance.
- This theoretical method is more suitable for the collector under certain conditions, i.e., intense solar radiation and small heated fluid mass flow rate.

ACKNOWLEDGMENT

We are using the conceptual knowledge to do some useful work for the benefi to four society. This work is being done in the guidance of Assistant professor Mr. Saumitra Sharma who showed confidence in me and showed me different approach to achieve my goal. I am thankful to work with him.

REFERENCES

[1] Hussein HMS, El-Ghetany HH, Nada SA (2006) Performance of wickless heat pipe flat plate solar collectors having different pipes cross sections geometries and filling ratios. Energy Convers Manag 47(11–12):1539–1549

[2] Hussein HMS, Mohamad MA, El-Asfouri AS (1999) Transient investigation of a thermosiphon flat plate solar collector. ApplThermEng 19(7):789–800

[3] Hussein HMS, Mohamad MA, El-Asfouri AS (1999) Optimization of a wickless heat pipe flat plate collector. Energy Convers Manag 40(18):1949–1961

[4] Xiao, Lan, et al. "Theoretical investigation on thermal performance of heat pipe flat plate solar collector with cross flow heat exchanger." Heat and Mass Transfer 48.7 (2012): 1167-1176.

[5] Hussein HMS (2002) Transient investigation of a two phase closed thermosiphon flat-plate solar water heater. Energy Convers Manag 43(18):2479–2492

[6] Hussein HMS (2003) Optimization of a natural circulation two phase closed thermosiphon flat plate solar water heater. Energy Convers Manag 44(14):2341–2352

[7] Hussein HMS (2007) Theoretical and experimental investigation of wickless heat pipes flat plate solar collector with cross flow heat exchanger. Energy Convers Manag 48(4):1266–1272

[8] Riffat SB, Doherty PS, Abdel Aziz EI (2000) Performance testing of different types of liquid flat plate collectors. Int J Energy Res 24(13):1203–1215

[9] Riffat SB, Zhao X, Doherty PS (2002) Analytical and numerical simulation of the thermal performance of 'mini' gravitational and 'micro' gravitational heat pipes. ApplThermEng 22(9):1047– 1068

[10] Riffat SB, Zhao X (2004) A novel hybrid heat pipe solar collector/CHP system—part I: system design and construction. Renew Energy 29(15):2217–2233

[11] Riffat SB, Zhao X (2004) A novel hybrid heat-pipe solar collector/CHP system—part II: theoretical and experimental investigations. Renew Energy 29(12):1965–1990

[12] Riffat SB, Zhao X, Doherty PS (2005) Developing a theoretical model to investigate thermal performance of a thin membrane heat-pipe solar collector

[13] Nada SA, El-Ghetany HH, Hussein HMS (2004) Performance of a two-phase closed thermosiphon solar collector with a shell and tube heat exchanger. ApplThermEng 24(13):1959–1968

[14] Abu-ZourAM, Riffat SB, Gillott M (2006) New design of solar collector integrated into solar louvers for efficient heat transfer. ApplThermEng 26(16):1876–1882

[15] Yu ZT, Hu YC, Hong RH, Cen KF (2005) Investigation and analysis on a cellular heat pipe flat solar heater. Heat Mass Transf 42(2):122–128

[16] Rittidech S, Wannapakne S (2007) Experimental study of the performance of a solar collector by closed-end oscillating heat pipe (CEOHP). ApplThermEng 27(11–12):1978–1985
[17] Rittidech S, Donmaung A, Kumsombut K (2009) Experimental study of the performance of a circular tube solar collector with closed-loop oscillating heat-pipe with check valve (CLOHP/CV). Renew Energy 34(10):2234–2238
[18] Esen M, Esen H (2005) Experimental investigation of a two-phase closed thermosiphon solar water heater. Sol Energy 79(5):459–468
[19] Faca ˜o J, Oliveira AC (2005) the effect of condenser heat transfer on the energy performance of a plate heat pipe solar collector. Int J Energy Res 29(10):903–912
[20] Azad E (2008) Theoretical and experimental investigation of heat pipe solar collector. Exp Thermal Fluid Sci 32(8):1666–1672
[21] Azad E (2009) Performance analysis of wick-assisted heat pipe solar collector and comparison with experimental results. Heat Mass Transf 45(5):645–649
[22] Chi SW (1976) Heat pipe theory and practice. Hemisphere Publishing Corp, Washington
[23] Sodha MS (2006) Performance evaluation of solar PV/T system: an experimental validation. Sol Energy 80:751–759